Journal of Molecular Structure 1268 (2022) 133647

Contents lists available at ScienceDirect

Journal of Molecular Structure

journal homepage: www.elsevier.com/locate/molstr

Synthesis of benzimidazole derivatives containing amide bond and biological evaluation as acetylcholinesterase, carbonic anhydrase I and II inhibitors

Zuhal Alım[a], Turgay Tunç[b,*], Nadir Demirel[a], Aslıhan Günel[a], Nurcan Karacan[c]

[a] Department of Chemistry, Faculty of Arts and Sciences, University of Kırşehir Ahi Evran, Kırşehir 40100, Turkey
[b] Department of Chemistry Engineering, Faculty of Engineering University of Kırşehir Ahi Evran, Kırsehir 40100, Turkey
[c] Department of Chemistry, Faculty of Arts and Sciences, Gazi University, Ankara 06500, Turkey

ARTICLE INFO

Article history:
Received 15 February 2022
Revised 15 June 2022
Accepted 30 June 2022
Available online 5 July 2022

Keywords:
Acetylcholinesterase
Benzimidazole
Carbonic anhydrase
Inhibition
Molecular docking

ABSTRACT

Acetylcholinesterase (AChE) and carbonic anhydrase I (CA-I) and II (CA-II) are two vital metabolic enzymes. AChE inhibitors are seen as target molecules in drug development studies for Alzheimer's treatment. CA inhibitors are target molecules for treating many diseases from glaucoma to cancer. For this reason, it is crucial to identify new AChE and CA inhibitors. In this study, four benzimidazole acetamide derivatives were synthesized and their inhibition effects were investigated against human erythrocyte carbonic anhydrase I (hCA-I), II (hCA-II), and AChE. IC_{50} values of **9a-10b** were determined in the range of 0.936 to 17.07 µM for AChE. IC_{50} values of **9a–10b** for hCA-I were found as 7.21 µM, 4.72 µM, 6.08 µM, 8.23 µM, respectively. On the other hand, IC_{50} values of **9a–9b** for hCA-II were found as 8.64 µM, 7.07 µM, 4.12 µM, 5.93 µM, respectively. According to IC_{50} values, **9a**–**10b** molecules exhibited strong inhibition effects for AChE and hCAI, II. Also, Molecular docking studies were carried out to explain the binding interaction of **9a**–**10b** with AChE, hCA-I, and hCA-II.

1. Introduction

The benzimidazole derivatives are widely used clinically therapeutic agents [1–7]. They are one of the most valuable and influential structures in medicinal chemistry [8–11]. They have an essential role in drug discovery because benzimidazoles have numerous bioactivities, such as anti-protozoal, antimicrobial, anti-inflammatory, analgesic, antioxidant, anthelmintic, anti-hypertensive, anti-cancer, anti-human cytomegalovirus and anti-influenza activity [12–19]. Some benzimidazole derivatives have been reported to have significant antibacterial activity [20–26]. Benzimidazole derivatives containing amide bonds [27] provided a beneficial linkage in synthetic and medicinal chemistry [28] due to the bond's classical geometry and planar properties. Compounds containing amide bonds are used in many clinical studies for metabolic disorders [29], inflammatory diseases [30], hypertension [31], and cancer [32].

Carbonic anhydrase (CA) (EC 4.2.1.1) regulates the acidity of the chemical environment to prevent damage to body functions [33]. Due to this critical physiological function, numerous studies have been carried out on CAs. CA-I and CA-II are the most studied isoenzymes.CA-I is expressed in erythrocytes and the gastrointestinal tract, whereas CA-II is expressed in almost all tissues. CA-I and CA-II are involved in critical metabolic functions, such as gas exchange and ion transport [34]. Since CA isoenzymes are associated with many diseases, from glaucoma to cancer and even osteoporosis, CA inhibitors are target molecules in drug design studies [35].

Acetylcholinesterase (AChE; E.C.3.1.1.7) is an essential metabolic enzyme that catalyzes the hydrolysis of acetylcholine to acetic acid and choline [36]. Inhibitors of this enzyme have been effective in clinical applications as anti-Alzheimer's drugs in treating moderate Alzheimer's disease (AD). For this reason, the synthesis of new compounds containing amide bonds that will provide improved central nervous system penetration and microglial activation with fewer side effects becomes very important [27,37,38]. To date, a large number of CA and AChE inhibitors have been identified and included in clinical practice. However, the high side effects of these inhibitors have led to the need to identify new and effective CA and AChE inhibitors [35,39]. In this study, we investigated the inhibition effects of four new benzimidazole derivatives containing amide bond **9a–10b** (Scheme 1) against hCA-I, hCA-II, and AChE.

* Corresponding author.
E-mail address: ttunc@ahievran.edu.tr (T. Tunç).

https://doi.org/10.1016/j.molstruc.2022.133647
0022-2860/

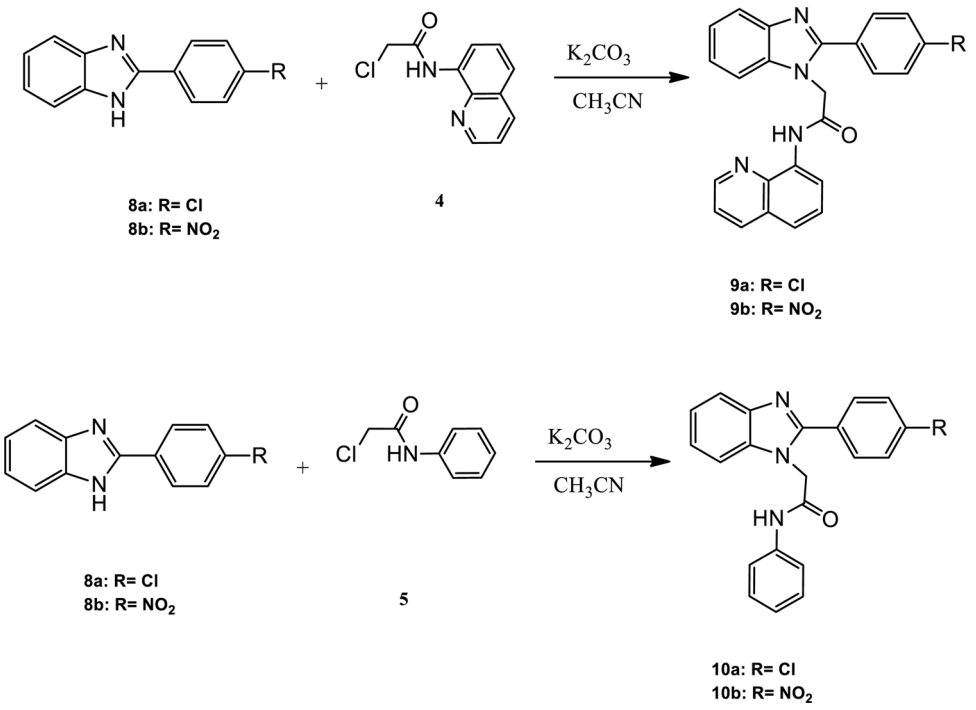

Scheme 1. Synthesis of benzimidazole derivatives containing amide bond.

2. Experimental

2.1. Materials

All solvents and reagents were purchased commercially available. DMF was dried before use. IR spectra were recorded on a Nicolet-6700 ATR-FT-IR spectrophotometer in the 4000– 400 cm^{-1} regions, and melting points were measured using a Thermo Fisher Scientific Electrothermal 9100 apparatus. ^{13}C-NMR (1 MHz) spectra and ^{1}H-NMR (400 MHz) spectra were collected on a Bruker Ultrashield spectrometer at room temperature with TMS, and solvent Mass spectra were recorded with Thermo Scientific TSQ Quantum Access Max LC-MS spectrometers in methanol/ acetonitrile mixture. Optical rotations were recorded using an ANTON PAAR MCP100 model polarimeter.

2.2. 2-(2-(4-chlorophenyl)-1H-benzo[d]imidazol-1-yl)-N-(quinolin-8-yl)acetamide
9a

2-(4-chlorophenyl)-1H-benzimidazole (0.32 g, 1.40 mmol), 2-chloro-N-(quinolin-8-yl)acetamide (0.31 g, 1.40 mmol) and K_2CO_3 (0.58 g, 4.20 mmol) were dissolved in DMF (15 mL). The mixture was refluxed at 150 °C for 48 h. At the end of the reaction, the mixture was cooled to room temperature and water was added. The mixture was extracted three times with ethyl acetate (3 × 10 mL), dried with sodium sulphate and evaporated and crude solid was washed with cold methanol to give **9a** as off-white solid; m.p.246–247 °C; IR (KBr, cm^{-1}) 3308 (νNH, m), 3049 (νC-H ring, m), 2938 (νCH_2,m), 1673(νC=O, s), 1599 (νC=C ring, s), 1575(νC=N in ring, s), 1488 (δ CH_2), 1454 (δN-H), 1320 (νC-N), 1281(δ ring), 1106(δ ring); ^{1}H-NMR ($CDCl_3$, 400 MHz), δ 5.13(s, 2H, -CH_2), 7.33–7.56(m, 8H, Ar-H), 7.79–7.81 (d, J = 9 Hz, 2H, Ar-H), 7.92–7.94(d, J = 8Hz, 1H, Ar-H), 8.13–8.15 (d, J = 8Hz, 1H, Ar-H), 8.57–8.58 (d, J = 4Hz, 1H, Ar-H), 8.73–8.75 (d, J = 8Hz, 1H, Ar-H), 10.17 8 (s, 1 H, CONH); ^{13}C-NMR ($CDCl_3$, 100 MHz), δ 49.16, 110.01, 116.97, 120.67, 121.93, 122.78, 123.61, 123.77, 124.52, 127.19, 127.94, 133.32, 135.58, 136.19, 136.29, 138.37, 143.41, 148.53, 14.67, 151.56, 162.38, 164.45; LC-MS (m/z): 412.99 [M+H] (calc. 412.87). (Figs. S1–S4).

2.3. 2-(2-(4-nitrophenyl)-1H-benzo[d]imidazol-1-yl)-N-(quinolin-8-yl)acetamide
9b

This compound was prepared in a similar method that was used to obtain compound **9a** from 2-(4-nitrophenyl)-1H-benzimidazole (0.35 g, 1.46 mmol), 2-chloro-N-(quinolin-8-yl)acetamide (0.32 g, 1.46 mmol) and K_2CO_3 (0.61 g, 4.38 mmol) to give **9b** as off-white solid; m.p.246–248 °C; IR (KBr, cm^{-1})· 3235 (νNH, m), 3054 (νC-H ring, m), 2930 (νCH_2,m), 1660(νC=O, s), 1599(νC=C ring,s), 1534(νasNO_2 ring, s), 1488(δ CH_2), 1460(δN-H), 1380 ((νsNO_2), 1339(νC-N), 1254(δ ring); ^{1}H-NMR ($CDCl_3$, 400 MHz), δ 5.18(s, 2H, -CH_2), 7.40–7.58(m, 6H), 7.95–7.97 (d, J = 8 Hz, 1H, Ar-H), 8.07–8.10(d, J = 12Hz, 2H, Ar-H), 8.17–8.19 (d, J = 8Hz, 1H, Ar-H), 8.37–8.39 (d, J = 12Hz, 2H, Ar-H), 8.62–8.63 (d, J = 4Hz, 1H,Ar-H), 8.72–8.74 (d, J = 8Hz, 1H, Ar-H),10.21(s, 1 H, CONH); ^{13}C-NMR ($CDCl_3$, 100 MHz), δ 49.10, 109.91, 116.84, 120.05, 121.55, 122.64, 123.30, 123.90, 124.52, 127.11, 127.83, 127.99, 129.12, 129.37, 130.70, 133.07, 135.96, 136.06, 136.69, 138.34, 143.08, 148.51, 153.08, 164.80; LC-MS (m/z): 424.03 [M+H] (calc. 423.42). (Figs. S5–S8).

2.4. hCA-I and hCA-II inhibitory assay

CA-I and II isoenzymes were purified from human erythrocytes in one step using CNBr-activated Sepharose-4B-L-tyrosine sulfanilamide affinity chromatography as in our previous studies [35,40,41]. Quantitative protein determination in purification steps was done by the Bradford method [42]. The purity of isoenzymes was checked with the SDS-PAGE method [43] as in our previous studies [35,44,45]. CA-I and CA-II isoenzymes purified by affinity chromatography dialyzed against 50 mM Tris-SO4 (pH 7.4) buffer overnight. After dialysis, isoenzymes were stored in small fractions

of one milliliter at -80°C for use in inhibition studies. In inhibition studies, the activities of hCA-I and hCA-II isoenzymes were performed according to the esterase activity measurement method [46]. This method is based on the hydrolysis of CA isoenzymes to p-nitro phenyl acetate, which turns into p-nitro-phenol and acetic acid. Accordingly, p-nitrophenyl acetate was used as the substrate in the inhibition studies. The formation of p-nitrophenol from p-nitrophenyl acetate was monitored by measuring the absorbance at 348 nm, 25 °C using a spectrophotometer. The enzyme unit was calculated using the absorption coefficient ($\varepsilon = 5.4 \times 10^3$ M^{-1} cm^{-1}) of p-nitrophenyl acetate at 348 nm. Inhibition effects of **9a**–**10b** molecules were determined on the esterase activity of hCA-I and II isoenzymes. For this, hCA-I and hCA-II activities were measured at least five concentrations of each **9a**–**10b** molecule. Percent activity values of both isoenzymes at five different inhibitor concentrations were calculated. The control activity of the enzyme was accepted as 100%, and inhibitor concentrations were graphed versus percent activity of both isoenzymes. IC_{50} values were determined from the equations of these graphs (Fig. S9). Acetazolamide (AZA) was used as the reference inhibitor for hCA-I and hCA-II isoenzymes.

2.5. AChE inhibitory assay

The AChE (CAS no. 9000-81-1) enzyme was commercially available from Sigma-Aldrich. AChE activity in inhibition studies was performed according to the spectrophotometric method of Ellman et al. [47] as in our previous studies [39,40]. In this method, the acetylcholinesterase catalyzes the conversion of acetylthiocholine to thiocholine and acetic acid. The thiocholine that formed reacts with the DTNB (Ellman's reagent, 5.5-dithio-bis-(2-nitrobenzoic acid). As a result of this reaction, a yellow colored 5-thio-2-nitrobenzoic acid complex is formed. The color intensity of the resulting colored compound is measured spectrophotometrically [48]. Accordingly, acetylthiocholine iodide was used as a substrate in inhibition studies. The color intensity of the resulting colored compound was measured at 412 nm. AChE activity was measured at least five concentrations for **9a**–**10b** compounds to determine the inhibition effects of **9a**–**10b** on AChE activity. The control activity of the enzyme was accepted as 100%, and inhibitor concentrations were graphed against Activity%. IC_{50} values were determined from the equations of these graphs (Fig. S10). Tacrine (TAC) was used as the reference inhibitor for AChE.

2.6. Molecular docking study

The crystal structures *of tetronarce californica* acetylcholinesterase (PDB ID: 1ACJ) [49], hCA-I (PDB ID: 1AZM) [50], and hCA-II (PDB: 2H4N) [51] were obtained from RCSB Protein Data Bank.

The structure of the enzymes was prepared using the Protein Preparation Wizard module (Schrödinger Release, 2021-1) [52]. Protein structures were corrected by adding hydrogen atoms and missing residues, assigning bond orders and bond length, creating disulphide bonds, fixing the charges, refining the loop with Prime, and finally minimizing by using the OPLS-2005force field at pH of 7.4.

The compounds' conversion was optimized at the PM6 level in the water phase using the polarizable continuum solvation method (iefpcm) using Gaussian 03 software. Later, the compounds' possible ionization and tautomeric states were prepared using the LigPrep module embedded Schrödinger suite using the OPLS_2005 force field.

The receptor Grid Generation panel was used for determining the position and size of the active site of the receptor structure by excluding co-crystallized ligands such as tacrine and acetazolamide.

Docking analysis was performed by Glide in Schrödinger platform [52] at extra-precision mode (XP) using OPLS_2005 force field. After evaluating the determined XP docking scores, the ligands' best poses were re-docked using the induced fit docking module of Maestro. To this end, a fully flexible docking methodology for both receptor residues and docked ligands was used by Glide XP (extra precision)-Induced Fit Docking (IFD) algorithm, which was implemented with the Prime module under Schrodinger molecular modeling package [52]. The accuracy of the molecular docking method was validated by redocking of co-crystallized ligand into the crystal structure of the receptor.

The docking method was verified using the redocking test. Cognate ligands were redocked into corresponding binding pockets. RMSD values of the redocked cognate ligands were observed to be in the range of 0.26–0.46 Å, confirming the accuracy and feasibility of the docking method.

2.7. In silico *ADME analysis*

The compounds' pharmacokinetics profile was predicted using the Qikprop v3.6 module embedded Schrödinger platform [52]. QikProp helps analyze the pharmacokinetics and pharmacodynamics of the compounds by accessing the drug-like properties. QikProp module calculates pharmacokinetic properties and descriptors such as a hydrophobic component of the solvent-accessible surface area (FOSA), the hydrophilic part of the solvent-accessible surface area (FISA), the weakly polar component of the solvent-accessible surface area (WPSA), predicted polarizability (QPpolrz), octanol/water partitioning coefficient (QPlogP), aqueous solubility (QPlogS), predicted Caco-2 cell permeability (QPPCaco), predicted skin permeability (QPlogKp), human serum albumin binding (QPlogKhsa), predicted IC_{50} value for blockage of HERG K^+ channels (QPlogHERG), brain/blood partition coefficient (QPlogBB), predicted apparent MDCK cell permeability QPMDCK, predicted central nervous system activity CNS and others.

3. Results and discussion

3.1. Chemistry

2-chloro-N-(quinol-8-yl) acetamide and 2-chloro-N-(phenyl) acetamide were synthesized according to the literature [53,54]. 2-(4-nitrophenyl)-1H-benzo[d]imidazole and 2-(4-chlorophenyl)-1H-benzo[d]imidazole was synthesized according to the procedure recorded in literature [21] in polyphosphoric acid at 130–140 °C from *o*-phenylene diamine and *p*-Cl, *p*-NO_2-substitüe benzoic acid.

Compounds **9a** and **9b** were synthesized by the reaction of benzimidazole derivatives (**8a** and **8b)** with the 2-chloro-N-(quinol-8-yl) acetamide in CH_3CN in the presence of K_2CO_3 as the base. **10a** and **10b** were synthesized by reactions of benzimidazole derivatives (**8a, 8b)** with the 2-chloro-N-(phenyl) acetamide, according to the literature [55,56].

NMR spectra of the 2-(2-(4-chlorophenyl)-1H-benzo[d]imidazol-1-yl)-*N*-(quinolin-8-yl)acetamide and 2-(2-(4-nitrophenyl)-1*H*-benzo[d]imidazol-1-yl)-*N*-(quinolin-8-yl) acetamide, are very simple as expected. *p*-Cl and *p*-NO_2 substitute derivatives gave CONH peak at 10.17 ppm and at 10.21 ppm as a singlet, respectively. The methylene proton of the amide unit gave singlet at 5.13 ppm and 5.18 ppm, respectively. The observed NMR spectrum of the compounds **9a** and **9b** in the aromatic region is consistent with the structures. The other spectral (IR, ^{13}C, and LCMS) data were consistent with the structures. (Figs. S1–S8).

Table 1
The IC_{50} values of the compounds for AChE, hCA-I and hCA-II.

Compounds	For AChE		For hCA-I		For hCA-II	
	IC_{50} (μM)	R^2	IC_{50} (μM)	R^2	IC_{50} (μM)	R^2
9a	0.936	0.9194	7,21	0,9421	8,64	0,8423
9b	7.632	0.9521	4,72	0,9647	7,07	0,9648
10a	10.43	0.9510	6,08	0,9917	4,12	0,8327
10b	17.07	0.9503	8,23	0,9673	5,93	0,7877
Tacrine	0.697	0.9218	-	-	-	-
Acetazolamide	-	-	0.536	0.9834	0.281	0.9877

*Tacrine was used as a standard inhibitor for AChE.
* Acetazolamide (AZA) was used as a standard inhibitor for hCA-I and hCA-II.

3.2. Biology

3.2.1. AChE, hCA-I, and hCA-II inhibition activity

The summary of IC_{50} values is given in Table 1. The inhibition effects of the **9a–10b** were compared with the reference inhibitors acetazolamide (AZA) and tacrine (TAC) for hCA isoenzymes and AChE, respectively. The inhibition effects of the molecules were determined by the IC_{50} values, which are defined as the inhibitor concentration that halves the enzyme activity. A low IC_{50} value indicates a high inhibitory activity. IC_{50} values for AChE of **9a–10b** molecules were determined as 0.936 μM, 7.632 μM, 10.43 μM, 17.07 μM, respectively. These values were compared with the reference inhibitor, TAC. Although compounds **9b, 10a, and 10b** exhibited a lower inhibition activity than TAC, compound **9a** (0.936 μM) showed closed inhibition activity as TAC (0.697 μM). The inhibitory effects of the **9a–10b** on hCA-I and hCA-II were compared with the reference inhibitor AZA. As for hCA-I, IC_{50} values for **9a–10b** were found as 7.21μM, 4.72μM, 6.08μM, 8.23μM, respectively. The IC_{50} values for the hCA-II isoenzyme of **9a–10b** molecules were found as 8.64 μM, 7.07 μM, 4.12 μM, 5.93 μM, respectively. These benzimidazole derivatives were weak inhibitors compared with reference inhibitor AZA but had inhibitory activity on hCA-I and hCA-II at micromolar concentrations. **9b** showed the most substantial inhibitory effect for hCA-I, while **10a** had the most substantial inhibitory effect for hCA-II. In our study, molecular docking studies were also carried out to explain the binding interaction of **9a-10b** with hCA-I, hCA-II, and AChE.

3.3. Molecular docking studies

The crystal structure of *tetronarce californica* acetylcholinesterase (PDB ID: 1ACJ) was chosen for docking because it contains tacrine as cognate ligand, used as a reference drug for in vitro biological assay. Similarly, the crystal structure of hCA-I (PDB ID: 1AZM) and hCA-II (PDB: 2H4N) containing AZA as a cognate ligand was chosen for docking analysis.

The compounds were docked into the active site of the enzymes (AChE, (hCA-I, hCA-II), at which cognate ligands bind. The compounds' most negative Glide/IFD docking scores are listed in Table 2. 2-D interaction diagram and detailed binding mode of the best pose of the compounds for the AChE, CA-I, and hCA-II enzymes are illustrated in Figs. 1–3.

Docking results show that all compounds have a higher docking score than the corresponding cognate ligand "tacrine" (-13.888 kcal/mol). Tacrine is tightly bound to the binding pocket via pi-pi stacking to Trp84, Phe330, and Tyr442 and cation-pi interaction to Phe330 (Fig. 1). **9a** has the best docking scores (-17.727 kcal/mol) and is the most effective inhibitor against AChE. **9a** formed three hydrogen bonds with Asp72, Tyr 121, His 440, pi-cation, pi-pi stacking interaction with Trp84 and Phe330, and a halogen bond with Gly117. Tacrine and **9b** are both bound to the indole ring of Trp84 and phenyl ring of Phe330, which are

Table 2
Glide/IFD binding score (kcal/mol) of the compounds.

Compounds	IFD Docking Score (kcal/mol)		
	AChE	hCAI	hCAII
9a	-17.727	-6.489	-6.442
10a	-16.516	-6.771	-7.454
9b	-16.455	-8.467	-5.751
10b	-16.221	-7.041	-4.416
Tacrine	-13.888	-	-
Acetazolamide	-	-9.257	-8.605

critical amino acid residues involved in the mechanism of inhibition [57]. **9a** was surrounded by primarily hydrophobic interaction with Tyr70, Val71, Tyr130, Trp279, Tyr334, Trp432, Met436, Ile439, Tyr442, and Ile444. **9b, 10a,** and **10b** have similar docking scores against AChE **(Figs. S11–S13).** Chloro and nitro groups afforded additional halogen bonding with Gly117 and hydrogen bonding with Asp72, Tyr121, and Tyr130. AChE enzymes.

At the active hCA-I site, zinc(II) cation is liganted by His94 and His119 and hydroxide ion/water molecule with tetrahedral geometry. The crystal structure of CA-sulfonamide complexes shows that mono anion sulfonamide displaces zinc-bound hydroxide to form a stable enzyme-inhibitor complex and interacts with Thr199 via hydrogen bonds [58]. Sulfonamides have ionizable protons (NH_2, pK_a= 7.4) at the physiological pH [59], but our compounds have not (NH, pKa ∼ 14). However, docking analysis shows that our neutral compounds are bonded to the zinc(II) cation via an O atom of the NO_2 group (Zn-O bond length is about 2.0 A) or N donor atom of the imidazole ring (Zn–N bond length is about 2.4 A).

9b (-8.467 kcal/mol) has a better docking score than **10b** (-7.041 kcal) but not better than reference acetazolamide (-9.257 kcal/mol) into hCA-I (Figs. 2, S14). They are coordinated to zinc(II) cation with an O atom of the nitro group (Zn-O bond length is about 2.0 Å). They also have pi-cation interaction with His200 and Hie67 and hydrophobic interaction with Val62, Phe91, Ala121, Leu131, Ala132, Ala136, Leu141, Val143, Pro202, Try204, Trp209 of the residue of hCA-I.

10a (-6.771 kcal/mol) and **9a** (-6.489 kcal/mol) showed less negative docking score than **9b** and **10b Figs. S15 and S16)**. They are not coordinated to Zn(II) cation (Zn-Cl length between 3.1 and 4.4 Å). They are oriented toward the hydrophobic region to form hydrophobic interaction in the active site of hCA-I. **10a** also formed a halogen bond with Thr1199 and pi-pi stacking with His200; however, **9a** made pi-pi stacking with Phe 91.

Generally, the compounds showed a lower glide score against hCA-II than the corresponding hCA-I and a lower binding score than acetazolamide (-8.605). **10a** (-7.454 kcal mol) has the best docking scores against hCA-II (Fig. 3). 10a and **9a (Fig. S17)** are coordinated to zinc(II) cation with an N donor atom of the imida-

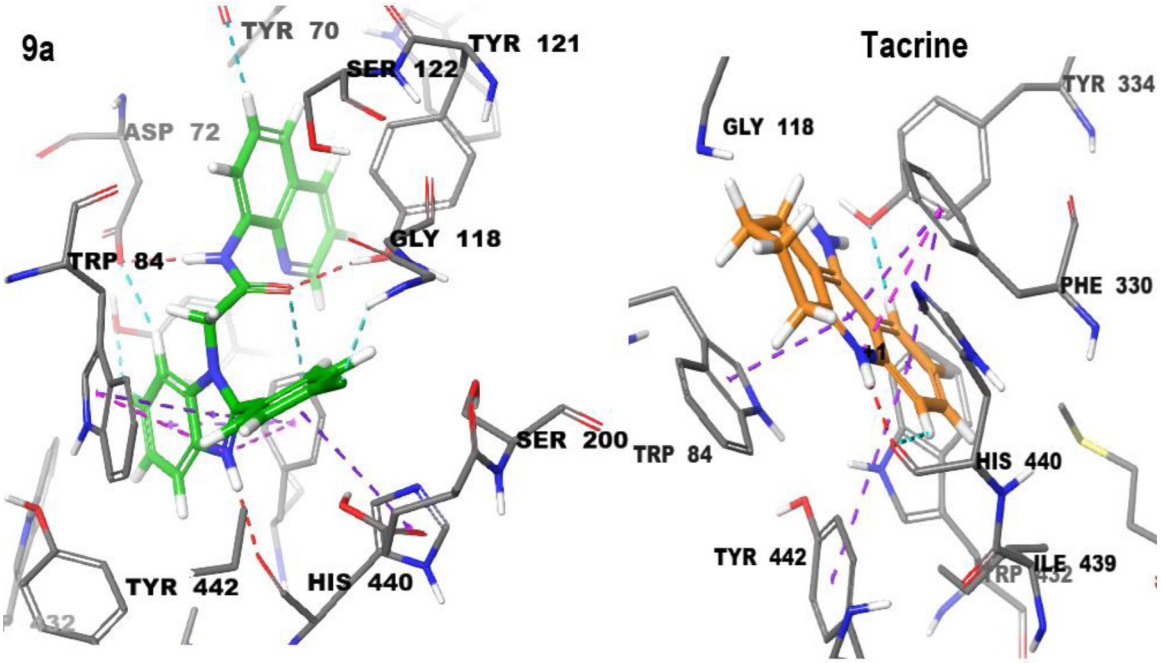

Fig. 1. The best pose of the **9a** and tacrine in the active site of AChE (PDB ID: 1ACJ).

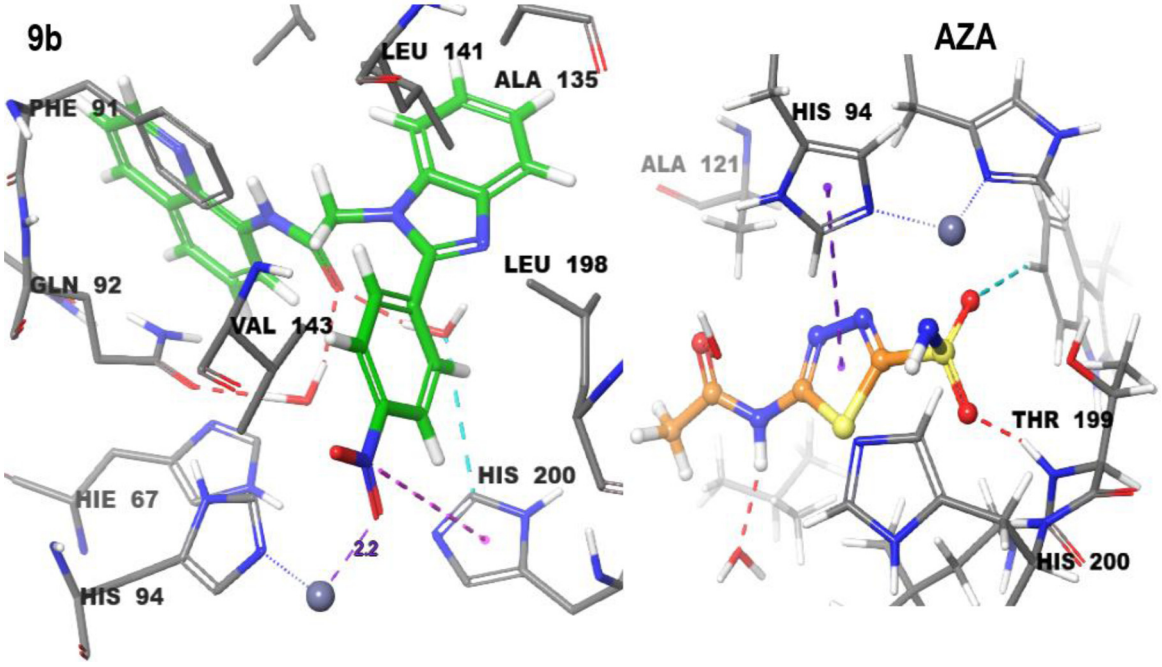

Fig. 2. The best pose of the **9b** and acetazolamide in the active site of hCA-I (PDB ID:1AZM).

zole ring (Zn–N bond length is about 2.2 Å). **10a** also has halogen bonding interaction with Asn62 and pi-pi stacking interaction with His96; however, **9a** has pi-pi interaction with Phe131 and hydrogen bonding interaction with Gln92.

10b (-4.416 kcal/mol) exhibited the lowest docking score among other compounds against hCA-II **(Fig. S18). 10b** and **9b** are coordinated to zinc(II) cation with an O atom of the nitro group (Zn–O bond length is about 2.2 Å). **9b** also has pi-pi interaction with Phe131 and hydrogen bond interaction with Asn67 (Fig. S19). All these four ligands showed slightly different inhibition activities experimentally, but the meaningful differences were not observed through binding energies for them.

3.4. ADME Study

In drug design, it is vital to determine the ADME properties of drug-like molecules. For this purpose, Qikprop module embedded Schrödinger package was utilized. Some descriptors and ADME (absorption, distribution, metabolism, and excretion) properties of the compounds are given in Table 2.

As can be seen, ADME calculations showed that synthesized ligands quietly obey the rule of five without any considerable violations; that is, compounds can be predicted to follow Lipinski's rule (MW $<$ 500, QPlogPo/w $<$ 5, donor HB $\leq$ 5, accptHB $\leq$ 10) and to have drug-like properties. Also, the compounds are more likely to

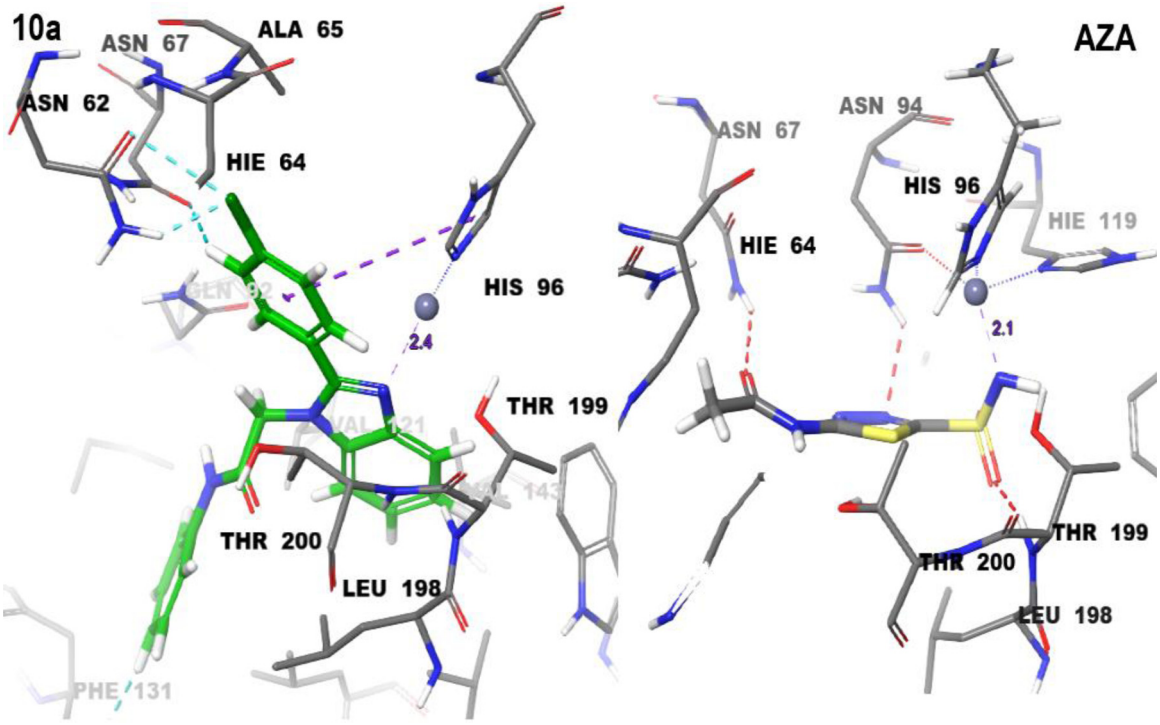

Fig. 3. The best pose of the **10a** and acetazolamide in the active site of hCA-II (PDB ID:2H4N).

Table 3
Some descriptors and drug-likeness properties of the compounds.

	Standard	9a	10a	9b	10b
FOSA	0.0–750.0	17.72	15.67	22.99	26.63
FISA	7.0–330.0	62.75	52.73	173.5	146.9
WPSA	0.0–175.0	71.23	71.23	0	0
volume	500–2000	1258.84	1074.12	1322.61	1165.13
QPpolrz	13.0 / 70.0	47.64			
MW	130.0/725.0	412.87	361.83	423.43	372.38
DHB	0.0/ 6.0	1	1	1	1
AHB	2.0 / 20.0	5	4	6	5
QPlogP	-2 / 6.0	5.57	4.79	4.51	4.05
QPlogS	-6.5 / -0.5	-7.21	-5.42	-7.23	-5.97
QPPCaco	25 >	2516.63	3132.18	224	400.41
QPlogKp	-8.0 / -1.0	-0.41	-0.61	-2.34	-2.09
QPlogKhsa	-1.5 / 1.5	0.93	0.65	0.84	0.63
QPlogHERG	-5 <	-7.57	-5.99	-8.01	-7.12
QPlogBB	-3.0 / 1.2	-0.11	0.08	-1.65	-1.21
QPPMDCK	25 >	3306.71	4173.63	98.20	183.95
CNS	-2 / +2	0	1	-2	-2
RuleofFive		1	0	0	0
RuleofThree		1	0	1	1

be orally available because the number of violations of Jorgensen's three rules (QPlogS > -5.7, QP PCaco > 22 nm/s, total primary metabolites < 7) is acceptable. In addition, Caco-2 cell permeability, skin permeability, IC_{50} value for HERG K^+ channels obstruction, brain-blood barrier partition coefficient, MDCK cell permeability, human serum albumin binding, and central nervous system activity values of the compounds are within range, which made the compounds of choice for acetylcholinesterase and carbonic anhydrase proteins (Table 3).

4. Conclusion

Four benzimidazole derivatives containing amide bond (**9a–10b**) were synthesized, and inhibition properties of the compounds were investigated against AChE, hCA-I, and hCA-II. **9a–10b** showed good inhibition activity against AChE, hCA-I, and hCA-II. Molecular docking analysis for the compounds showed that all compounds had good binding affinity against AChE receptors. **9a** showed the best inhibition activity against AChE. Our compounds showed less activity than cognate ligand acetazolamide for the hCA-I and hCA-II. Generally, all compounds exhibit lower activity against hCA-II than the corresponding hCA-I. The ADME (absorption, distribution, metabolism, and excretion) studies indicated that **9a, 9b, 10a,** and **10b** have high gastrointestinal absorption, no brain-blood barrier (BBB) permeation, and less skin permeation. In conclusion, the research results will contribute to the development of new and effective AChE and CA inhibitors.

Declaration of Competing Interest

The authors declare no conflict of interest. Zuhal Alım: Determination of biological properties of compounds. Turgay Tunç: Synthesis of benzimidazole derivatives. Nadir Demirel: Synthesis of benzimidazole derivatives. Aslıhan Günel: Determination of biological properties of compounds. Nurcan Karacan: Molecular docking studies.

Supplementary materials

Supplementary material associated with this article can be found, in the online version, at doi:10.1016/j.molstruc.2022.133647.

References

[1] M.R. Grimmet, K.T. Potts, in: Comprehensive Heterocyclic Chemistry, 4, Pergamon Oxford, 1984, p. 345. Ed..
[2] M.R. Grimmet, I. Shinkai, in: Comprehensive Heterocyclic Chemistry II, 3, Pergamon Oxford, 1996, p. 77. Ed..
[3] P.N. Preston, Synthesis, reactions, and spectroscopic properties of benzimidazoles, Chem. Rev. 74 (1974) 279–314.
[4] R.J. Sundberg, R.B. Martin, Interactions of histidine and other imidazole derivatives with transition metal ions in chemical and biological systems, Chem. Rev. 74 (1974) 471–517.
[5] C. Nájera, M. Yus, Chiral benzimidazoles as hydrogen bonding organocatalysts, Tetrahedron Lett. 56 (2015) 2623–2633.

[6] V.N. Khose, M.E. John, A.D. Pandey, A.V. Karnik, Chiral benziimidazoles and their applications in stereodiscrimination processes, Tetrahedron Asymmetry 28 (2017) 1233–1289.
[7] J.A. Asensio, E.M. Sanchez, P. Gómez-Romero, Proton-conducting membranes based on benzimidazolepolymers for high-temperature PEMfuelcells. A chemical quest, Chem. Soc. Rev. 39 (2010) 3210–3239.
[8] J.E. Payne, C. Bonnefous, K.T. Symons, P.M. Nguyen, M. Sablad, N. Rozenkrants, Y. Zhang, L. Wang, N. Yazdani, A.K. Shiau, S.A. Noble, P. Rix, T.S. Rao, C.A. Hassig, N.D. Smith, Discovery of dual inducible/neuronal nitric oxide synthase (iNOS/nNOS) inhibitor development candidate 4-((2-cyclobutyl-1H-imidazo[4,5-b]pyrazin-1-yl)methyl)-7,8-difluoroquinolin-2(1H)-one (KD7332) part 2: identification of a novel, potent, and selective series of benzimidazole-quinolinone iNOS/nNOS dimerization inhibitors that are orally active in pain models, J. Med. Chem. 53 (2010) 7739–7755.
[9] H.S. Al-Muhaimeed, A parallel-group comparison of Astemizole and Loratadine for the treatment of perennial allergic rhinitis, J. Int. Med. Res. 25 (1997) 175–181.
[10] L.J. Scott, C.J. Dunn, G. Mallarkey, M. Sharpe, Esomeprazole: a review of its use in the management of acid-related disorders, Drugs 62 (2002) 1503–1538.
[11] M. Gaba, S. Singh, C. Mohan, Benzimidazole: an emerging scaffold for analgesic and anti-inflammatory agents, Eur. J. Med. Chem. 76 (2014) 494–505.
[12] D.A. Horton, G.T. Bourne, M.L. Sinythe, The combinatorial synthesis of bicyclic privileged structures or privileged substructures, Chem. Rev. 103 (2003) 893–930.
[13] M. Alamgir, D.S.C. Black, N. Kumar, Synthesis, reactivity and biological activity of Benzimidazoles, Heterocycl. Chem. 9 (2007) 87–118.
[14] H. Goker, S. Ozden, S. Yildiz, D.W. Boykin, Synthesis and potent antibacterial activity against MRSA of some novel 1,2-disubstituted-1H-benzimidazole-N-alkylated-5-carboxamidines, Eur. J. Med. Chem. 40 (2005) 1062–1069.
[15] R. Abraham, P. Periakaruppan, K. Mahendran, M. Ramanathan, A novel series of N-acyl substituted indole-linked benzimidazoles and naphthoimidazoles as potential anti-inflammatory, anti-biofilm and anti-microbial agents, Microb. Pathog. 114 (2018) 409–413.
[16] Z. Zhu, B. Lippa, D.J. Drach, L.B. Townsend, Design, synthesis, and biological evaluation of tricyclic nucleosides (dimensional probes) as analogues of certain antiviral polyhalogenated benzimidazole ribonucleosides, J. Med. Chem. 43 (2000) 2430–2437.
[17] T. Rath, M.L. Morningstar, P.L. Boyer, S.M. Hughes, R.W. Buckheitjr, C.J. Michejda, Synthesis and biological activity of novel nonnucleoside inhibitors of HIV-1 reverse transcriptase. 2-Aryl-substituted benzimidazoles, J. Med. Chem. 40 (1997) 4199–4207.
[18] M.T. Migawa, J.L. Girardet, J.A. Walker, G.W. Koszalka, S.D. Chamberlain, J.C. Drach, L.B. Townsend, Design, synthesis, and antiviral activity of α-nucleosides: D- and L-isomers of lyxofuranosyl- and (5-Deoxylyxofuranosyl)benzimidazoles, J. Med. Chem. 41 (1998) 1242–1251.
[19] J. Mann, A. Baron, Y. Opoku-Boahen, E. Johansson, G. Parkinson, L.R. Kelland, S. Neidle, A new class of symmetric bisbenzimidazole-based DNA minor groove-binding agents showing antitumor activity, J. Med. Chem. 44 (2001) 138–144.
[20] K. Sambanthamoorthy, A.A. Gokhale, W. Lao, V. Parashar, M.B. Neiditch, M.F. Semmelhack, I. Lee, C.M. Waters, Identification of a novel benzimidazole that inhibits bacterial biofilm formation in a broad-spectrum manner, Antimicrob. Agents Chemother. 55 (2011) 4369–4378.
[21] S.M. Abdel-Wahab, Z.K. Abdelsamii, H.A. Abdel-Fattah, A.S. Eletrawy, L.N. Dawe, T.R. Swaroop, P.E Georghiou, Synthesis of 2-Aryl- and 2-Haloarylbenzimidazole-*N*1-acetamido conjugates and a preliminary evaluation of their antifungal properties, ChemistrySelect 3 (2018) 8106–8110.
[22] P.S. Singu, S. Kanugal, S.A. Dhawale, C.G. Kumar, M. Ravindra, R.M. Kumbhare, Synthesis and pharmacological evaluation of some amide functionalized 1H-Benzo[d]imidazole-2-thiol derivatives as anti-microbial agents, ChemistrySelect 5 (2020) 117–123.
[23] M. Holiyachi, S.L. Shastri, B.M. Chougala, L.A. Shastri, S.D. Joshi, S.R. Dixit, H. Nagarajaiah, V.A. Sunagar, Design, synthesis and structure-activity relationship study of coumarin benzimidazole hybrid as potent antibacterial and anticancer agents, ChemistrySelect 1 (2016) 4638–4644.
[24] N.B. Reddy, V. Grigory, G.V. Zyryanov, G.M. Reddy, A. Balakrishna, A. Padmaja, V. Padmavathi, C.S. Reddy, J.R. Garcia, G. Sravya, Design and synthesis of some new benzimidazole containing pyrazoles and pyrazolyl thiazoles as potential anti-microbial agents, J. Heterocycl. Chem. 56 (2019) 589–596.
[25] Y. Shi, K. Jiang, R. Zheng, J. Fu, L. Yan, Q. Gu, Y. Zhang, F. Lin, Design, microwave-assisted synthesis and in vitro antibacterial and antifungal activity of 2,5-disubstituted benzimidazole, Chem. Biodivers. 16 (2019) e1800510.
[26] N. Obaiah, N.D. Bodke, S. Telkar, Synthesis of 3-[(1H-Benzimidazol-2-ylsulfanyl)(aryl)methyl]-4-hydroxycoumarin derivatives as potent bioactive molecules, ChemistrySelect 5 (2020) 178–184.
[27] M. Imran, F.A. Shah, H. Nadeem, A. Zeb, M. Faheem, S. Naz, A. Bukhari, T. Ali, S. Li, Synthesis and biological evaluation of benzimidazole derivatives as potential neuroprotective agents in an ethanol-induced rodent model, ACS Chem. Neurosci. 12 (2021) 489–505.
[28] M.E. Condon, E.W. Petrillo, D.E. Ryono, J.A. Reid, R. Neubeck, M. Puar, J.E. Heikes, E.F. Sabo, K.A. Losee, D.W. Cushman, M.A. Ondetti, Angiotensin-converting enzyme inhibitors: importance of the amide carbonyl of mercaptoacyl amino acids for hydrogen bonding to the enzyme, J. Med. Chem. 25 (19829) (1982) 250–258.
[29] M. Yu, M.M. Benjamin, S. Srinivasan, E.E. Morin, E.I. Shishatskaya, S.P. Schwendeman, A. Schwendeman, Battle of GLP-1 delivery technologies, Adv. Drug Deliv. Rev. 130 (2018) 113–130.
[30] M.G. Giovannini, C. Scali, C. Prosper, A. Bellucci, G. Pepeu, F. Casamenti, Experimental brain inflammation and neurodegeneration as model of Alzheimer's disease: protective effects of selective COX-2 inhibitors, Int. J. Immunopathol. Pharmacol. 16 (2003) 31–40.
[31] S.I. Sokol, A. Cheng, W.H. Frishman, C.S. Kaza, Cardiovascular drug therapy in patients with hepatic diseases and patients with congestive heart failure, J. Clin. Pharmacol. 40 (2000) 11–30.
[32] M. Brown, J.H. Clark, H.F. Sneddon, J. Sherwood, L. Summerton, A.J. Hunt, K. Kummerer, J. Hayler, J. Messinger, J. Moseley, Green and Sustainable Medicinal Chemistry; Methods, Tools and Strategies for the 21st Century Pharmaceutical Industry, Royal Society of Chemistry, 2016.
[33] C. Geers, G. Gros, Carbon dioxide transport and carbonic anhydrase in blood and muscle, Physiol. Rev. 80 (2000) 681–715.
[34] P.Y. Hu, D.E. Roth, L.A. Skaggs, P.J. Venta, R.E. Tashian, P. Guibaud, W.S. Sly, A splice junction mutation in intron 2 of the carbonic anhydrase II gene of osteopetrosis patients from Arabic countries, Hum. Mutat. 1 (1992) 288–292.
[35] Z. Alım, Z. Köksal, M. Karaman, Evaluation of some thiophene-based sulfonamides as potent inhibitors of carbonic anhydrase I and II isoenzymes isolated from human erythrocytes by kinetic and molecular modelling studies, Pharmacol. Rep. 72 (2020) 1738–1748.
[36] H. Shirinzadeh, E. Dilek, Z. Alım, Evaluation of naphthalenylmethylen hydrazine derivatives as potent inhibitors on, antiatherogenic enzymes, paraoxonase i and acetylcholinesterase activities, ChemistrySelect 7 (2022) e202104489.
[37] R.S. Doody, Therapeutic standards in Alzheimer disease, Alzheimer Dis. Assoc. Disord. 13 (1999) 20–26.
[38] V. Tumiatti, A. Minarini, M.L. Bolognesi, A. Milelli, M. Rosini, C. Melchiorre, Tacrine derivatives and Alzheimer's disease, Curr. Med. Chem. 17 (2010) 1825–1838.
[39] Z. Köksal, Z. Alım, S. Bayrak, I. Gülçin, H. Özdemir, Investigation of the effects of some sulfonamides on acetylcholinesterase and carbonic anhydrase enzymes, J. Biochem. Mol. Toxicol. 33 (2019) e22300.
[40] T. Tunç, Z. Alım, Synthesis of new schiff bases and assessment of their *in vitro* biological effects on acetylcholinesterase and carbonic anhydrase isoenzymes activities, Russ. J. Org. Chem. 57 (2021) 247–254.
[41] E. Karakılıç, Z. Alım, M. Emirik, A. Baran, Some characteristics of new and innovative COX inhibitor derivatives: potent hCA-I and hCA-II inhibitors supported by molecular docking studies, Appl. Organomet. Chem. 36 (2022) e6537.
[42] M.M. Bradford, A rapid and sensitive method for the quantitation of microgram quantities of protein utilizing the principle of protein dye binding, Anal. Biochem. 72 (1976) 248–254.
[43] U.K. Laemmli, Cleavage of structural proteins during the assembly of the head of bacteriophage T4, Nature 227 (1970) 680–685.
[44] Z. Alım, N. Kilinç, M.M. Işgör, B. Şengül, Ş. Beydemir, Some anti-inflammatory agents inhibit esterase activities of human carbonic anhydrase isoforms I and II: an *in vitro* study, Chem. Biol. Drug Des. 86 (2015) 857–863.
[45] Z. Alım, 1H-indazole molecules reduced the activity of human erythrocytes carbonic anhydrase I and II isoenzymes, J. Biochem. Mol. Toxicol. 32 (2018) e22194.
[46] J.A. Verpoorte, S. Mehta, J.T. Edsall, Esterase activities of human carbonic anhydrases B and C, J. Biol. Chem. 242 (1967) 4221–4229.
[47] G.L. Ellman, K.D. Courtney, V. Andres, R.M. Featherstone, A new and rapid colorimetric determination of acetylcholinesterase activity, Biochem. Pharmacol. 7 (1961) 88–95.
[48] C. Türkeş, M. Arslan, Y. Demir, Ç. Liridon, A.R. Nixha, Ş. Beydemir, synthesis, biological evaluation and in silico studies of novel N-substituted phthalazine sulfonamide compounds as potent carbonic anhydrase and acetylcholinesterase inhibitors, Bioorg. Chem. 89 (2019) 103004.
[49] M. Harel, I. Schalk, L. Ehret-Sabatier, F. Bouet, M. Goeldner, C. Hirth, P.H. Axelsen, I. Silman, J.L. Sussman, Proc. Natl. Acad. Sci. U.S.A 90 (1993) 9031–9903.
[50] S. Chakravarty, K.K. Kannan, Drug-protein interactions. Refined structures of three sulfonamide drug complexes of human carbonic anhydrase I enzyme, J. Mol. Biol. 243 (1994) 298–309.
[51] C.A. Lesburg, C. Huang, D.W. Christianson, C.A. Fierke, Histidine –>carboxamide ligand substitutions in the zinc binding site of carbonic anhydrase II alter metal coordination geometry but retain catalytic activity, Biochemistry 36 (1997) 15780 -1579.
[52] Schrödinger Release (2021-1): SiteMap, LigPrep v5.3; Glide v8.8; Maestro v4.3, Qikprop v3.6 LLC, New York, NY, 2021.
[53] Y. Zhang, X. Guo, W. Si, L. Jia, X. Qian, Ratiometric and water-soluble fluorescent zinc sensor of Carboxamidoquinoline with an Alkoxyethylamino chain as receptor, Org. Lett. 10 (2008) 473–476.
[54] R.V. Patel, P.K. Patel, P. Kumari, D.P. Rajani, K.H. Chikhalia, Synthesis of benzimidazolyl-1,3,4-oxadiazol-2ylthio-N-phenyl (benzothiazolyl) acetamides as antibacterial, antifungal and antituberculosis agents, Eur. J. Med. Chem. 53 (2012) 41–51.
[55] R. Sawant, D. Kawade, Synthesis and biological evaluation of some novel 2-phenyl benzimidazole-1-acetamide derivatives as potential anthelmintic agents, Acta Pharm. 61 (2011) 353–361.
[56] Z. Rouifia, M. Rbaab, A.S. Abousalemc, F. Benhibaa, T. Laabaissia, H. Ouddaa, B. Lakhrissib, A. Guenboure, I. Waradf, A. Zarrouke, Synthesis, characterization

and corrosion inhibition potential of newly benzimidazole derivatives: combining theoretical and experimental study, Surf. Interfaces 18 (2020) 100442.
[57] T. Vello, Acetylcholinesterase: mechanism of catalysis and inhibition, Curr. Med. Chem. 1 (2001) 155–170.
[58] P.A. Boriack-Sjodin, S. Zeitlin, H.H. Chen, L. Crenshaw, S. Gross, A. Dantanarayana, P. Delgado, J.A. May, T. Dean, D.W. Christianson, Structural analysis of inhibitor binding to human carbonic anhydrase II, Protein Sci. 7 (1998) 2483–2489.
[59] M. Remko, Molecular structure, pKa, lipophilicity, solubility and absorption of biologically active aromatic and heterocyclic sulfonamides, J. Mol. Struct. 944 (2010) 34–42.